Atmos. Chem. Phys. Discuss., 11, 29441–29477, 2011
www.atmos-chem-phys-discuss.net/11/29441/2011/
doi:10.5194/acpd-11-29441-2011

Atmospheric Chemistry and Physics Discussions

Gas-particle partitioning of atmospheric Hg(II) and its effect on global mercury deposition

H. M. Amos[1], D. J. Jacob[1,2], C. D. Holmes[3], J. A. Fisher[1], Q. Wang[2], R. M. Yantosca[2], E. S. Corbitt[1], E. Galarneau[4], A. P. Rutter[5], M. S. Gustin[6], A. Steffen[4], J. J. Schauer[7], J. A. Graydon[8], V. L. St. Louis[8], R. W. Talbot[9], E. S. Edgerton[10], and E. M. Sunderland[2,11]

[1]Department of Earth and Planetary Sciences, Harvard University, Cambridge, MA, USA
[2]School of Engineering and Applied Sciences, Harvard University, Boston, MA, USA
[3]Department of Earth System Science, University of California, Irvine, CA, USA
[4]Air Quality Research Branch, Environment Canada, Toronto, Ont., Canada
[5]Civil and Environmental Engineering Department, Rice University, Houston, TX, USA
[6]Department of Natural Resources and Environmental Sciences, University of Nevada, Reno, NV, USA
[7]Department of Civil and Environmental Engineering, University of Wisconsin, Madison, WI, USA
[8]Department of Biological Sciences, University of Alberta, Edmonton, Alberta, Canada

[9]Department of Earth and Atmospheric Sciences, University of Houston, Houston, TX, USA
[10]Atmospheric Research & Analysis, Inc., Cary, NC, USA
[11]Department of Environmental Health, Harvard University, Boston, MA, USA

Received: 19 October 2011 – Accepted: 20 October 2011 – Published: 31 October 2011

Correspondence to: H. M. Amos (amos@fas.harvard.edu)

Published by Copernicus Publications on behalf of the European Geosciences Union.

ACPD
11, 29441–29477, 2011

Abstract

Atmospheric deposition represents a major input of mercury to surface environments. The phase of mercury (gas or particle) has important implications for its removal from the atmosphere. We use long-term observations of reactive gaseous mercury (RGM), particle-bound mercury (PBM), fine particulate matter ($PM_{2.5}$), and temperature at five sites in North America to derive an empirical gas-particle partitioning relationship $\log_{10}(K^{-1}) = (10 \pm 1) - (2500 \pm 300)/T$ where $K = (PBM/PM_{2.5})/RGM$ with PBM and RGM in common mixing ratio units, $PM_{2.5}$ in $\mu g\,m^{-3}$, and T in Kelvin. This relationship is in the range of previous work but is based on far more extensive data from multiple sites. We implement this empirical relationship in the GEOS-Chem global 3-D Hg model to partition divalent mercury (Hg(II)). The resulting gas-phase fraction of Hg(II) ranges from over 90 % in warm air with little aerosol to less than 10 % in cold air with high aerosol. Hg deposition to high latitudes increases because of more efficient scavenging of particulate Hg(II) by snow. Model comparison to Hg observations at surface sites suggests that subsidence from the free troposphere (warm air, low aerosol) is a major factor driving the seasonality of RGM, while elevated PBM is mostly associated with high aerosol loads. This and other model updates, including the correction of an outstanding algorithm error, to wet deposition improve the simulation of Hg wet deposition fluxes in the US relative to the previous version of the model. The observed wintertime minimum in wet deposition fluxes is attributed to inefficient snow scavenging of gas-phase Hg(II).

1 Introduction

Mercury (Hg) is a naturally occurring metal that can cause adverse health effects on humans and wildlife (Clarkson and Magos, 2006; Mergler et al., 2007; Scheulhammer et al., 2007). Human exposure in developed countries is mainly through contaminated fish consumption (Mahaffey et al., 2004, 2009). Deposition to oceans has increased

ACPD
11, 29441–29477, 2011

since the pre-industrial era due to anthropogenic emissions (Mason and Sheu, 2002; Sunderland and Mason, 2007). Mercury is released to the atmosphere mainly as elemental mercury (Hg(0)), though combustion processes also emit divalent mercury (Hg(II)). Hg(0) in the atmosphere can eventually be oxidized to Hg(II). Hg(II) compounds have low vapor pressure ($HgCl_2$ 8.99×10^{-3} Pa at 20 °C, HgO 9.20×10^{-12} Pa at 25 °C), partition between the gas and particle phases, and are thus readily removed by removed by wet and dry deposition (Schroeder and Munthe, 1998; Lin et al., 2006). The phase partitioning of Hg(II) has important implications for deposition because gases and particles are deposited by different physical processes and at different rates (Seinfeld and Pandis, 2006). Hg(0) has a high vapor pressure (0.18 Pa at 20 °C (Schroeder and Munthe, 1998)) and its sorption to particles is thought to be negligible (Seigneur et al., 1998). Limited measurements suggest Hg(0) may be present in particulate Hg in heavily polluted urban areas (Sakata and Marumoto, 2002; Xiu et al., 2009). Here we use long-term observational records of speciated Hg to develop a mechanistic parameterization of Hg(II) gas-particle partitioning, and apply it to a simulation of Hg deposition using the GEOS-Chem global 3-D chemical transport model (CTM).

There is considerable uncertainty regarding the atmospheric chemistry of Hg (Hynes et al., 2009) and atmospheric measurement methods (Gustin and Jaffe, 2010). Despite these uncertainties, atmospheric Hg(II) compounds are thought to be semi-volatile and hence partition between the gas phase and particulate matter (PM) (Petersen et al., 1995; Seigneur et al., 1998). Current measurements use an operationally defined method for quantifying reactive gaseous mercury (RGM) and fine fraction (<2.5 µm) particle-bound mercury (PBM) (Lamborg et al., 1995; Keeler et al., 1995; Landis et al., 2002). Rutter and Schauer (2007b) investigated the mechanism of Hg partitioning in the air by fitting urban and laboratory data for RGM and PBM to a temperature-dependent expression for Hg(II) sorption onto PM smaller than 2.5 µm in diameter ($PM_{2.5}$). This approach is similar to parameterizations previously developed for other semi-volatile species including polycyclic aromatic hydrocarbons (Yamasaki et

ACPD
11, 29441–29477, 2011

al., 1982; Pankow, 1987) and secondary organic compounds (Pankow, 1994; Odum et al., 1996; Chung and Seinfeld, 2002).

Little was known about Hg(II) gas-particle partitioning prior to the work of Rutter and Schauer et al. (2007a, b). Earlier models of atmospheric Hg included parameterizations for the sorption of dissolved Hg species to soot particles suspended in cloud water (Petersen et al., 1998, Seigneur et al., 2001; Bullock and Brehme, 2002; Dastoor and Larocque, 2004) based on experimental results from Petersen et al. (1995) and Seigneur et al. (1998). In more recent years, models of atmospheric Hg have taken various approaches to treating Hg(II) gas-particle partitioning. Vijayaraghavan et al. (2008) implemented the temperature-dependent Hg(II) gas-particle partitioning formulation of Rutter and Schauer (2007b) into a regional model over the United States for a two-month (August–September) simulation. Vijayaraghavan et al. (2008) found that including Hg(II) gas-particle partitioning was most important in regions of high PM. Previous versions of GEOS-Chem have either assumed atmospheric Hg(II) to be entirely gas-phase (Selin et al., 2007, 2008) or assumed 50/50 gas-particle (Holmes et al., 2010; Soerensen et al., 2010; Corbitt et al., 2011).

Here we use long-term RGM and PBM observations at five sites in North America to derive an empirical gas-particle Hg(II) partitioning coefficient as a function of $PM_{2.5}$ and temperature, following the approach of Rutter and Schauer (2007b) but with a much larger data set. We show that a single parameterization can describe the Hg(II) partitioning across sites, and compare the resulting GEOS-Chem simulation to observations. The implications for global Hg deposition are discussed.

2 Hg(II) gas-particle partitioning

Data sets of RGM and PBM were obtained from five sites: Reno, Thompson Farm, Outlying Landing Field (Pensacola), Experimental Lakes Area, and Milwaukee (Table 1). The Experimental Lakes site includes 4 yr of data, the Reno site 2 yr and the others one year or slightly less. Figures 1 and 2 show the spatial and seasonal (monthly) distributions of the data and are discussed in Sect. 4.

ACPD
11, 29441–29477, 2011

All Hg measurements were collected with Tekran mercury analyzers (2537A, 1130, and 1135 units). Air is drawn through a heated (50 °C) impactor which removes coarse (>2.5 µm) particles from the air stream, then through a KCl-coated annual denuder to collect RGM, followed by a quartz fiber filter to collect PBM (Landis et al., 2002). The filter and denuder are sequentially heated to 800 °C and 500 °C, respectively, to thermally desorb the collected RGM and PBM. The desorbed RGM and PBM are sequentially reduced to Hg(0) as they pass through an 800 °C pyrolyzer and are finally analyzed as Hg(0) by cold vapor atomic fluorescence spectroscopy (CVAFS). Previous work has suggested that there are artifacts associated with PBM collection and there are interferences with the collection of RGM on the denuders, and surrogate methods suggest that the annular denuders do not have 100 % collection efficiency (Lynam and Keeler, 2005; Lyman et al 2007; Malcolm and Keeler, 2007; Rutter et al., 2008a; Gustin and Jaffe, 2010; Lyman et al., 2010). Lyman and Gustin (2009) reported that two Tekran instruments sampling side-by-side disagreed by 8 ± 40 % for RGM and 71 ± 41 % for PBM.

Keeping the limitations of the Tekran instrument in mind, we use them in the absence of other information. We parameterize the partitioning of Hg(II) between the gas and particle phases with a partitioning coefficient K (Rutter and Schauer, 2007a, b):

$$K = (\mathrm{PBM}/\mathrm{PM}_{2.5})/\mathrm{RGM} \quad (1)$$

where RGM and PBM are atmospheric mixing ratios (ppq) and $\mathrm{PM}_{2.5}$ is the dry mass concentration ($\mu g\, m^{-3}$). It is assumed that Eq. (1) represents equilibrium between the gas and particle phases of atmospheric Hg(II), and that the major Hg(II) compounds measured as RGM and PBM have similar volatilities so that a single equilibrium constant is applicable. Normalization by $\mathrm{PM}_{2.5}$ makes the additional assumption that uptake is proportional to the aerosol mass concentration, although adsorption to a solid aerosol phase would be equivalent if a fixed scaling is assumed between the volume and area of the aerosol (Yamasaki et al., 1982; Pankow, 1987; Rutter and Schauer, 2007a, b). Restriction to fine aerosol ($\mathrm{PM}_{2.5}$) in Eq. (1) is consistent with the size cut-off of the Tekran instrument used to measure these Hg species.

ACPD
11, 29441–29477, 2011

Previous applications of Eq. (1) to PAHs and SOA have found a van't Hoff type of relationship between K and the local temperature T (Yamasaki et al., 1982; Pankow, 1987):

$$\log_{10}(K^{-1}) = a + \frac{b}{T} \quad (2)$$

where a and b are coefficients. Figure 3 shows the daily data from the sites in Table 1 fit to Eq. (2). Confidence intervals (95 %) for the slope and intercept are constructed using a bootstrap method. All RGM and PBM observations are averaged over mid-day hours (10:00–16:00 local time) when vertical mixing is strongest and the air mass being sampled is more likely to be homogenous. $PM_{2.5}$ data are 24-h averages as no higher temporal resolution is available. Use of 24-h average RGM and PBM data, as compared to daytime averages, does not significantly change the results. Pankow et al. (1993) suggested that relative humidity (RH) affected gas-particle partitioning of semi-volatile organic compounds. We tested this by performing a multivariate regression, $\log_{10}(K^{-1}) = a + b/T + c \cdot \mathrm{RH}$, and found no significant dependence on RH at any of the sites.

Table 2 lists the regression fits for individual sites. We tested them for statistical distinctness following Galarneau et al. (2006). Reno, Thompson Farm, and Experimental Lakes are statistically indistinct, as are Milwaukee, Pensacola, Thompson Farm, and Experimental Lakes. Reno is distinct from Pensacola and Milwaukee. Differences in aerosol composition between sites would be expected to affect the fits (Rutter and Schauer, 2007a, b) but no obvious relationship was found. The regression fit for the combined data set (all sites) is $\log(K^{-1}) = (10 \pm 1) - (2500 \pm 300)/T$ ($r^2 = 0.49$), and will be used in the analysis below.

The regression coefficients from this work fall in the envelope of those reported by Rutter and Schauer (2007b) for urban measurements using a filter-based method vs. a Tekran instrument (Fig. 3). Our derived coefficients are statistically indistinguishable from their laboratory data for partitioning of $HgCl_2$ with adipic acid aerosol and differ most from their partitioning of $HgCl_2$ to dry, synthesized $(NH_4)_2SO_4$ aerosol (Table 2).

ACPD
11, 29441–29477, 2011

Rutter and Schauer (2007b) hypothesized that the difference in partitioning between their filter-based method and the Tekran instrument could reflect a Tekran sampling artifact associated with internally heating the instrument to 50 °C but this remains speculative. Filter-based methods are also prone to artifacts (Lyman et al., 2009). The filter-based method used by Rutter and Schauer (2007b) relied on KCl coated filters to collect RGM, which Lyman et al. (2009) show to have poor collection efficiency after a week. Both of these potential sampling artifacts would lead to higher RGM measurements by the Tekran than by the filter-based method, consistent with the differences in partitioning shown here.

3 GEOS-Chem model simulation

We use version 9-01-01 of the GEOS-Chem Hg coupled atmosphere-ocean-land model (http://www.geos-chem.org/), which includes an atmosphere from Holmes et al. (2010), a surface ocean from Soerensen et al. (2010), and a land surface from Selin et al. (2008). The simulation is conducted for 2004–2009 with GEOS-5 assimilated meteorological and surface data from the NASA Global Modeling and Assimilation Office (GMAO). The years 2004–2006 are used for initialization and 2007–2009 for analysis. The original GEOS-5 data have 1/2° × 2/3° horizontal resolution and 72 vertical levels. The horizontal resolution is degraded here to 4° × 5° for input to GEOS-Chem for computational expediency. The GEOS-Chem simulation transports three Hg species in the atmosphere: elemental Hg (Hg(0)), semi-volatile divalent Hg (Hg(II)), and inert refractory particulate Hg (Hg(p)) (Selin et al., 2007). Atmospheric Hg(0)/Hg(II) redox chemistry follows Holmes et al. (2010), with oxidation of Hg(0) by Br atoms and photoreduction of Hg(II) in liquid cloud droplets.

Direct emissions of Hg(II) and Hg(p) in GEOS-Chem are entirely of anthropogenic origin, while emissions of Hg(0) are from both natural and anthropogenic sources (Schroeder and Munthe, 1998). Anthropogenic emissions are from Pacyna et al. (2010) for the year 2005. There is considerable ambiguity surrounding anthropogenic Hg(p)

ACPD
11, 29441–29477, 2011

in the literature, which confounds the interpretation of how it should treated in models and compared to Tekran measurements of PBM. Hg(p) in the emission inventories is intended to represent chemically inert Hg that is incorporated into soot or fly ash particles (J. Pacyna, personal communication, 2011). It is not clear that heating to 800 °C in the Tekran instrument would be sufficient to desorb such mercury from the collection filter. Considering it as PBM in the model would contradict the assumption that PBM is semi-volatile. For purpose of comparing with observations, we thus assume that gas-phase and particle-phase Hg(II) in the model correspond to RGM and PBM respectively, and that Hg(p) would not be measured as PBM. The sensitivity to this latter assumption is discussed in Sect. 4. We also assume that Hg(0) does not significantly partition into the aerosol on account of its high volatility (Schroeder and Munthe, 1998; Seigneur et al., 1998) and thus does not contribute to PBM.

The Hg(0):Hg(II):Hg(p) speciation from coal combustion in the Pacyna et al. (2010) emission inventory is 50:40:10. Observations of power plant plumes (Edgerton et al., 2006; Weiss-Penzias et al., 2011; ter Schure et al., 2011) indicate much lower Hg(II)/Hg(0) ratios, suggesting fast in-plume reduction of Hg(II) (Seigneur et al., 2003; Lohman et al., 2006). We find in GEOS-Chem that a large decrease in the fraction of Hg emitted as Hg(II) or Hg(p) from coal combustion improves consistency with observed RGM and PBM concentrations of Fig. 2. A 90:7:3 speciation from coal combustion is implemented to accommodate this constraint. A 90 % contribution from Hg(0) is slightly larger than observed by Edgerton et al. (2006) (mean 84 %), but is not outside the range observed by Wang et al. (2010) (66–94 %) for coal-fired power plants. Similar corrections to the emission inventory have been implemented by Y. Zhang et al. (2011) (77:20:3) in a nested GEOS-Chem Hg simulation for North America to better match MDN wet deposition measurements and by Kos et al. (2011) (90:8:2) in the GRAHM global model to better match surface concentrations of RGM and PBM. The implicit inclusion of Hg(II) in-plume reduction in the model comes with the important caveats that a chemical mechanism has not been indentified (Lohman et al., 2006), and that there are significant uncertainties associated with both the speciation of anthropogenic

ACPD
11, 29441–29477, 2011

emission inventories (UNEP, 2008) and methods for measuring atmospheric Hg (Gustin and Jaffe, 2010).

Hg(II) in the model is partitioned between the gas and particle phases for the purpose of calculating deposition, using the parameterization from Sect. 2. Here, $PM_{2.5}$ is specified as the sum of sulfate, nitrate, ammonium, carbonaceous, and fine dust particle mass from archived GEOS-Chem monthly means of a full-aerosol simulation for the year 2007 (L. Zhang et al., 2011). The resulting Hg(II) particulate fraction in the model ranges from less than 10 % in warm environments with low aerosol to more than 90 % in cold environments with high aerosol (Fig. 4). Gas-particle partitioning of Hg(II) with sea-salt particles in the marine boundary layer is accounted for separately in GEOS-Chem as described by Holmes et al. (2010). Holmes et al. (2009, 2010) developed a more physical model for uptake of Hg(II) by sea-salt aerosol based on formation of Hg-Cl complexes (Clever et al., 1985; Hedgecock and Pirrone, 2001).

Dry deposition in GEOS-Chem is computed with a standard resistance-in-series scheme and is much faster for water-soluble gases than for particles (Wesely, 1990). RGM has been observed to have very high dry deposition velocities (0.4–7.6 $cm\,s^{-1}$) (Lindberg and Stratton, 1998; Poissant et al., 2004; Skov et al., 2006; Lyman et al., 2007, 2009) and so a negligibly small surface resistance is assumed for gaseous Hg(II) (Selin et al., 2007). Dry deposition of particulate Hg(II) follows the standard surface resistance formulation of Wesely (1990) as implemented by Wang et al. (1998). Simulated global annual mean dry deposition velocities are 0.93 $cm\,s^{-1}$ for gaseous Hg(II) and 0.11 $cm\,s^{-1}$ for particulate Hg(II) + Hg(p).

Wet deposition of Hg(II) and Hg(p) in GEOS-Chem includes scavenging from moist convective updrafts as well as rainout and washout by large-scale precipitation (Liu et al., 2001). Gaseous Hg(II) is scavenged as $HgCl_2$ with a Henry's law constant of $1.4 \times 10^6\,M\,atm^{-1}$ (Lindqvist and Rodhe, 1985). Recent improvements from Wang et al. (2011) are included, which allow rainout and washout to occur in the same grid box and take into account the change in aerosol size distribution over the course of a precipitation event. Gaseous Hg(II) and particulate Hg(II) + Hg(p) are retained by

ACPD
11, 29441–29477, 2011

supercooled water during freezing (Holmes et al., 2010). There is observational evidence that falling snow is inefficient at scavenging RGM (Keeler et al., 2005; Sigler et al., 2009; Lombard et al., 2011; Mao et al., 2011) and so below-cloud scavenging of gaseous Hg(II) by snow is suppressed. By contrast, particulate Hg is scavenged by falling snow in the same manner as its aerosol carriers. We conducted a ^{222}Rn-^{210}Pb simulation (Liu et al., 2001) to test the model representation of aerosol deposition. ^{210}Pb is produced by decay of terrigenic ^{222}Rn and attaches indiscriminately to aerosols, which are then removed by wet and dry deposition. We obtained a lifetime of tropospheric ^{210}Pb against deposition of 10.4 days, consistent with a value of about 9 days in previous global 3-D model studies supported by comparisons to ^{222}Rn and ^{210}Pb observations (Balkanski et al., 1993; Koch et al., 1996; Liu et al., 2001).

An important update in this study is to correct the washout of gases by rain in GEOS-Chem, as previous versions had an implementation error affecting the scavenging of highly soluble gases other than HNO_3 (and including gaseous Hg(II)). The GEOS-Chem washout scheme for gases had not been documented previously in the literature and we do so here (see Appendix), including the correction. After the correction we find that the global lifetime of tropospheric gaseous Hg(II) against wet deposition is reduced from 108 days to 46 days (the lifetime is relatively long because of the large fraction of the inventory in the upper troposphere).

A standard practice in environmental modeling of Hg is to adjust parameters within their uncertainty to fit global observations of Hg(0) concentrations and wet deposition fluxes (Selin et al., 2007; Holmes et al., 2010). To account for the changes made in the current version, the rate coefficient for atmospheric in-cloud reduction is reduced by 50 % relative to Holmes et al. (2010). We evaluated the model against the global set of land and cruise ship measurements from Holmes et al. (2010) and results are similar (not shown here). Our global budget of Hg is similar to that in Holmes et al. (2010) and Soerensen et al. (2010). Global tropospheric burdens are 3600 Mg Hg(0), 500 Mg Hg(II) (310 Mg gas and 190 Mg particulate), and 2 Mg refractory Hg(p). Net Hg(0) ocean evasion is 2900 Mg a^{-1} (14 Mmol a^{-1}), which is

ACPD
11, 29441–29477, 2011

consistent with Soerensen et al. (2010) and within the 90 % confidence intervals of 10–21 Mmol a^{-1} simulated by Sunderland and Mason (2007). On a global scale, dry deposition is 2500 Mg a^{-1} (56 % Hg(0) (land only), 43 % Hg(II), 1 % Hg(p)), wet deposition is 3000 Mg a^{-1} (99 % Hg(II), 1 % Hg(p)), and deposition of Hg(II) via sea salt is 1600 Mg a^{-1}.

4 Comparison to surface observations

Simulated annual mean Hg(0), RGM, and PBM show reasonable consistency with observed annual means (Fig. 1). RGM in the model is maximum over the western US where warm air with low aerosol subsides from the free troposphere (Selin and Jacob, 2008). PBM is maximum over the Midwest and eastern US where $PM_{2.5}$ concentrations and anthropogenic Hg emissions are high.

Simulated and observed monthly mean Hg(0), RGM, and PBM are compared in Fig. 2. The observed seasonality of Hg(0) at Thompson Farm, Experimental Lakes Area, and Pensacola in Fig. 2 is typical of northern mid-latitudes, with maximum in early spring and minimum in late summer/early fall. Photochemical destruction is likely the major process contributing to the summer decrease (Bergan and Rodhe, 2001; Selin et al., 2007; Holmes et al., 2010). The concentration of Hg(0) at Reno and Milwaukee is much greater and more variable than background continental concentrations and, likely reflecting local urban sources (Rutter et al., 2008b; Lyman and Gustin, 2009) that are not resolved by the coarse horizontal resolution of the model.

There is much greater spatial variability for observed RGM and PBM than for Hg(0), reflecting the difference in atmospheric lifetimes. An implication is that variability in RGM and PBM is not significantly driven by variability in Hg(0). Engle et al. (2010) previously examined the seasonality of speciated Hg at nine sites across central and eastern North America, and reported large site-to-site variability that they attributed to a complex combination of processes including local point sources, exchange between the boundary layer and the free troposphere, and coastal effects. Temperature and

ACPD
11, 29441–29477, 2011

aerosol concentrations would also play a role through the partitioning between RGM and PBM.

RGM concentrations are highest at Reno and Milwaukee in summer, both in the observations and in the model. The summer maximum at Reno is due to entrainment of RGM-rich free tropospheric air during deep diurnal mixed layer growth (Lyman and Gustin, 2009; Weiss-Penzias et al., 2009). This entrainment is associated with low aerosol concentrations and high temperatures, so that there is little associated enhancement of PBM. Lyman and Gustin (2009) suggest that the observed summer peak in PBM at Reno is due to extensive wildfire plumes during the summer of 2008 affecting the area (Arnott et al., 2008), and this is consistent with other observations of enhanced PBM during wildfires (Friedli et al., 2003a, b; Finley et al., 2009). The model does not capture this particulate event of wildfire enhancement. The elevated summer RGM at Milwaukee is due to regional anthropogenic sources in the Midwest (Rutter et al., 2008b), with a corresponding enhancement of PBM in winter when low temperatures cause this anthropogenic Hg(II) to be partitioned into the aerosol. The simulated seasonality of RGM is reasonably consistent with observations, but the model over predicts both RGM and PBM during the winter.

RGM and PBM at Thompson Farm and Experimental Lakes Area peak in winter-spring, both in the observations and the model. This seasonality in the model is due to the upper troposphere and lower stratosphere (UT/LS), which is thought to contain a large reservoir of Hg(II) (Swartzendruber et al., 2006; Faïn et al., 2009). Similar seasonality is found in model and observations for aerosol ^{7}Be, which is cosmogenically produced in the UT/LS and removed by deposition (Liu et al., 2001; Yoshimori, 2005; Muramatsu et al., 2008; Alegría et al., 2010). We find in the model that surface RGM and ^{7}Be have similar seasonal behavior; correlating the two in the observations would provide a test of UT/LS influence on surface Hg(II). At Pensacola, the spurious summer peak of RGM in the model appears to be due to excessively deep boundary layer mixing. That site is affected by sea breezes, which are not resolved by the model and would restrict boundary layer growth.

ACPD
11, 29441–29477, 2011

As discussed above, we have assumed that primary refractory Hg(p) simulated by the model is not measured as PBM, consistent with our general assumption that PBM is semi-volatile. Inclusion of Hg(p) would increase monthly mean model PBM by a factor of 1.4–3 (Experimental Lakes Area – Pensacola), degrading the agreement with observations. Even though Hg(p) is a negligible (<1 %) component of the global Hg budget in the model, it is relatively important in surface air over source regions. We previously speculated that refractory Hg(p) might not be desorbed from the aerosol collection filter of the Tekran instrument. In addition, field observations show that >2.5 µm diameter particles (not sampled by the Tekran instrument) can represent up to 68 % of total particulate Hg in polluted air and up to 37 % in rural air (Keeler et al., 1995; Gildemeister et al., 2005). Comparison of Tekran and filter-based sampling methods suggests that the Tekran instrument underestimates the total aerosol concentration (Talbot et al., 2011). Finally, the model assumption that Hg(p) is refractory could be flawed; if it were semi-volatile and behaving as Hg(II), its influence on surface concentrations would be much less because of losses from volatilization and reduction.

5 Implications for Hg deposition

Gas-particle partitioning impacts the global spatial distribution of Hg(II) deposition in the model. Figure 5 shows the relative difference in total Hg(II) deposition between the standard simulation using Eqs. (1–2) and a sensitivity simulation where all Hg(II) is deposited as a gas. The standard simulation includes all model updates described in Sect. 3. The effect is largest at high latitudes because particulate Hg(II) is scavenged by snow but gaseous Hg(II) is not. The competing effect of faster dry deposition of gaseous Hg(II) dominates only over dry regions of the subtropics. The effect over tropical and subtropical oceans is small because there is little non-sea-salt aerosol and so Hg(II) is either in the gas phase or in the sea-salt aerosol (which is treated the same in the two simulations).

ACPD
11, 29441–29477, 2011

The extensive wet deposition flux data from the Mercury Deposition Network (MDN, 2011) in the US has been used in previous GEOS-Chem studies to evaluate the model deposition (Selin et al., 2007, 2008; Selin and Jacob, 2008; Holmes et al., 2010). Uncertainty in the MDN measurements is 10–25 % (Gustin and Jaffe, 2010). Figure 6 compares model results to the MDN observed annual Hg wet deposition fluxes for 2007–2009. The model version presented here shows an improved ability to reproduce observed Hg wet deposition fluxes over the US, including the decreasing gradient from Southeast to Northeast and the seasonal phase and amplitude. This is an important result because the poor simulation of the MDN data in Holmes et al. (2010) argued against Br atoms serving as the main Hg(0) oxidant (better simulation was achieved using OH and O_3 as oxidants). Our improved simulation of the MDN data (still using Br as the Hg(0) oxidant) largely reflects improvements in the washout algorithm, including corrected washout of gas-phase Hg(II) and updated aerosol washout coefficients adopted from Wang et al. (2011).

Selin and Jacob (2008) pointed out that the dominant modes of variability in the MDN data over the eastern US are a latitudinal gradient and a seasonal variation that decreases in amplitude with increasing latitude. Figure 7 compares observed and simulated seasonal variations of Hg wet deposition over the eastern US as a function of latitude, for the standard simulation and for sensitivity simulations with Hg(II) depositing either entirely as a gas or as a particle. The sensitivity simulations illustrate the effect of Hg(II) phase on simulated wet deposition. The standard model is able to capture the observed seasonal patterns of wet deposition and, except over the Gulf of Mexico, their latitude-dependent amplitudes. The sensitivity simulation with all Hg(II) depositing as a particle and thus scavenged by snow shows significant overestimate of wet deposition in winter. This lends support to the notion that gaseous Hg(II) (~50 % of total Hg(II) over US in winter, see Fig. 4) is not efficiently scavenged by snow. However, questions remain as to the MDN collection efficiency of snow (Sanei et al., 2010; Fain et al., 2011).

ACPD
11, 29441–29477, 2011

6 Conclusions

We have used long-term measurements of reactive gaseous mercury (RGM) and particle-bound mercury (PBM) at five sites in North America to derive an empirical gas-particle Hg(II) partitioning coefficient as a function of $PM_{2.5}$ and temperature. A single parameterization is used to describe the Hg(II) partitioning across sites. We implemented this parameterization in the global 3-D GEOS-Chem Hg model, compared model results with measurements of speciated Hg and wet deposition fluxes over the US, and discussed the implications for global Hg deposition.

We fit the RGM and PBM observations to a temperature-dependent gas-particle Hg(II) partitioning coefficient of the form $\log_{10}(K^{-1}) = (10 \pm 1) - (2500 \pm 300)/T$ where $K = (\mathrm{PBM}/\mathrm{PM}_{2.5})/\mathrm{RGM}$; here PBM and RGM are in common mixing ratio units, $PM_{2.5}$ is in $\mu g\,m^{-3}$, and T is in Kelvin.

Implementation of this Hg(II) gas-particle partitioning in GEOS-Chem yields Hg(II) fractions in the particle phase ranging from more than 90 % in cold air masses with high aerosol burdens to less than 10 % in warm air with low aerosol. Relative to a model simulation assuming all Hg(II) to be in the gas phase, Hg(II) deposition is increased at high latitudes because particulate Hg is more efficiently scavenged by snow, and decreased at subtropical latitudes because particulate Hg is less efficiently dry deposited.

Additional updates implemented in this version of GEOS-Chem include improvements to the washout algorithm and a change in the Hg(0):Hg(II):Hg(p) emission speciation for fossil fuel combustion from 50:40:10 to 90:7:3 to account for assumed rapid in-plume reduction. As previously noted by Kos et al. (2011) and Y. Zhang et al. (2011), decreasing the Hg(II) emission fraction is necessary to avoid large model overestimate of PBM observations at North American sites. There is ambiguity about the nature of Hg(p) included in current anthropogenic emission inventories. If it represents refractory mercury embedded in soot or fly ash particles then it might not be operationally measured as PBM. If it semi-volatile and behaves as Hg(II), then it is inconsequential beyond the immediate source area because most Hg(II) is of secondary origin.

ACPD
11, 29441–29477, 2011

We compare model results to seasonal observations of Hg(0), RGM, and PBM at the five North American surface sites used to construct the $K(T)$ parameterization. Observations in Reno and Milwaukee show particularly large summertime RGM that we attribute to subsidence of free tropospheric air (Reno) and regional anthropogenic sources (Milwaukee). Observations in rural New Hampshire (Thompson Farm) and Ontario (Experimental Lakes Area) show spring maxima in RGM and PBM that we attribute to UT/LS influence. These maxima are correlated in the model with cosmogenic ^{7}Be, suggesting that ^{7}Be measurements would be of value to separate global and local contributions in RGM and PBM observations.

Compared to the previous version of GEOS-Chem (Holmes et al., 2010), our model shows an improved ability to reproduce observed Hg wet deposition fluxes over the US from the Mercury Deposition Network (MDN), including the decreasing gradient from Southeast to Northeast and the seasonal phase and amplitude. This is an important result because the poor simulation of the MDN data in Holmes et al. (2010) argued against Br atoms serving as the main Hg(0) oxidant (better simulation was achieved using OH and O_3 as oxidants). Our improved simulation of the MDN data (still using Br as the Hg(0) oxidant) largely reflects improvements in the washout algorithm. The wintertime minima in the MDN data are attributed to inefficient snow scavenging of gaseous Hg(II).

Appendix A

GEOS-Chem algorithm for washout of soluble gases by rain

Below-cloud scavenging (washout) of gases by rain in GEOS-Chem is determined by Henry's law equilibrium but can be also limited by mass transfer for highly soluble gases (Levine and Schwartz, 1982). The fraction F of gas scavenged from a grid box by washout over a time step Δt as determined by Henry's law equilibrium is

ACPD
11, 29441–29477, 2011

$$F = f\frac{K^* L_p RT}{1 + K^* L_p RT} \quad \text{(A1)}$$

Here f is the areal fraction of the grid box experiencing precipitation, K^* is the effective Henry's law constant (M atm^{-1}) including any dissociation and complexation equilibria in the aqueous phase, R is the universal gas constant, T is temperature, and L_p is the time-integrated rainwater content in the precipitating fraction of the grid box

$$L_p = \frac{P\Delta t}{f\Delta Z} \quad \text{(A2)}$$

where P (cm^3 water cm^{-2} surface s^{-1}) is the grid-averaged precipitation flux through the bottom of the grid box and ΔZ (cm) is the grid box thickness. For highly soluble gases, F may be limited by molecular diffusion to the raindrops. On the basis of the detailed mass transfer calculations by Levine and Schwartz (1982) for diffusion-limited uptake of HNO_3, a maximum value F_{max} for F is derived as

$$F_{max} = f[1 - \exp(-k'\frac{P}{f}\Delta t)] \quad \text{(A3)}$$

where k' (cm^{-1}) is a washout rate constant ($k' = 1$ cm^{-1}; Table 2 of Levine and Schwartz, 1982).

GEOS-Chem computes F and F_{max} locally for every precipitating grid box and time step. If $F \le F_{max}$, it is assumed that washout is limited by Henry's law and the change in mass Δm of the soluble gas due to washout over Δt is then computed as

$$\Delta m = -F m + m_T(1 - \frac{F}{f}) \quad \text{(A4)}$$

where m is the mass of the gas in the grid box and m_T is the cumulative mass of gas scavenged via precipitation from above and entering the top of the grid box over Δt and over the fraction f. Equation (A4) allows for partial re-evaporation of the mass

ACPD
11, 29441–29477, 2011

scavenged from above. If $F > F_{max}$, it is assumed that washout is limited by mass transfer as given by Eq. (A3) and Δm is then computed as

$$\Delta m = -F_{max} m + \beta \alpha m_T \quad \text{(A5)}$$

where α is the fraction of precipitation falling through the top of the gridbox that evaporates within the gridbox, and β is the fraction of this re-evaporation that involves total evaporation of raindrops (which releases the gas to the gridbox) rather than partial shrinkage (which does not). It is assumed that $\beta = 0.5$ for $\alpha < 1$ and $\beta = 1$ for $\alpha = 1$ (Liu et al., 2001).

Because of a coding error in GEOS-Chem, the algorithm described above was incorrectly executed in previous model versions so that washout of highly soluble gases ($F > F_{max}$) was underestimated except for HNO_3 (which was correct). This affected the scavenging of gaseous Hg(II), for which a Henry's law constant of 1.4×10^6 M atm^{-1} is assumed based on laboratory data for $HgCl_2$ (Lindqvist and Rodhe, 1985). Correcting the error, as done here in the standard simulation, increases the lifetime of gaseous Hg(II) in the troposphere from 108 days to 46 days.

Acknowledgements. This work was funded by the NSF Atmospheric Chemistry Program and AMS and NSF Graduate Fellowships to HMA. HMA would like to thank Lee T. Murray for helpful instruction on using the GEOS-Chem Be-Pb-Rn simulation. Funding for the collection of data at the Experimental Lakes Area was provided by NSERC, Environment Canada and Manitoba Hydro.

References

Alegria, N., Herranz, M., Idoeta, R., and Legarda, F.: Study of Be-7 activity concentration in the air of northern spain, J. Radioanal. Nucl. Ch., 286, 347–351, doi:10.1007/s10967-010-0710-6, 2010.

AMAP/UNEP: Technical Background Report to the Global Atmospheric Mercury Assessment, Arctic Monitoring and Assessment Programme/UNEP Chemical Branch, 159 pp., 2008.

ACPD
11, 29441–29477, 2011

Arnott, W., Gyawali, M., and Arnold, I.: Aerosol Extinction and Single Scattering Albedo Downwind of the Summer 2008 California Wildfires Measured With Photoacoustic Spectrometers and Sunphotometers From 355 nm to 1047 nm, Eos, 89, AGU Fall Meeting Supplement, Abstract A11D-0169, 2008.

Balkanski, Y. J., Jacob, D. J., and Gardner, G. M.: Transport and residence times of tropospheric aerosols inferred from a global three-dimensional simulation of Pb-210, J. Geophys. Res., 98, 20573–20586, 1993.

Bergan, T. and Rodhe, H.: Oxidation of elemental mercury in the atmosphere; constraints imposed by global scale modeling, J. Atmos. Chem., 40, 191–212, 2001.

Bullock, O. R. and Brehme, K. A.: Atmospheric mercury simulation using the CMAQ model: Formulation description and analysis of wet deposition results, Atmos. Environ., 36, 2135–2146, 2002.

Chung, S. H. and Seinfeld, J. H.: Global distribution and climate forcing of carbonaceous aerosols, J. Geophys. Res., 107, 4407, doi:10.1029/2001JD001397, 2002.

Clarkson, T. W. and Magos, L.: The toxicology of mercury and its chemical compounds, Crit. Rev. Toxicol. , 36, 609–662, 2006.

Clever, H. L., Johnson, S. A., and Derrick, M. E.: The solubility of mercury and some sparingly soluble mercury salts in water and aqueous-electrolyte solutions, J. Phys. Chem. Ref. Data, 14, 631–681, 1985.

Cole, A. S. and Steffen, A.: Trends in long-term gaseous mercury observations in the Arctic and effects of temperature and other atmospheric conditions, Atmos. Chem. Phys., 10, 4661–4672, doi:10.5194/acp-10-4661-2010, 2010.

Corbitt, E. S., Jacob, D. J., Holmes, C. D., Streets, D. G., and Sunderland, E. M.: Global source-receptor relationships for mercury deposition under present-day and 2050 emissions scenarios, Environ. Sci. Technol., in review, 2011.

Corn, M., Montgome, T. L., and Esmen, N. A.: Suspended particulate matter – seasonal variation in specific surface areas and densities, Environ. Sci. Technol., 5, 155–158, doi:10.1021/es60049a001, 1971.

Dastoor, A. P. and Larocque, Y.: Global circulation of atmospheric mercury: A modeling study, Atmos. Environ., 38, 147–161, doi:10.1016/j.atmosenv.2003.08.037, 2004.

Edgerton, E. S., Hartsell, B. E., and Jansen, J. J.: Mercury speciation in coal-fired power plant plumes observed at three surface sites in the southeastern US, Environ. Sci. Technol., 40, 4563–4570, doi:10.1021/es0515607, 2006.

ACPD
11, 29441–29477, 2011

Engle, M. A., Tate, M. T., Krabbenhoft, D. P., Schauer, J. J., Kolker, A., Shanley, J. B., and Bothner, M. H.: Comparison of atmospheric mercury speciation and deposition at nine sites across central and eastern North America, J. Geophys. Res., 115, D18306, doi:10.1029/2010jd014064, 2010.

Faïn, X., Obrist, D., Hallar, A. G., McCubbin, I., and Rahn, T.: High levels of reactive gaseous mercury observed at a high elevation research laboratory in the Rocky Mountains, Atmos. Chem. Phys., 9, 8049–8060, doi:10.5194/acp-9-8049-2009, 2009.

Faïn, X., Obrist, D., Pierce, A., Barth, C., Gustin, M. S., and Boyle, D. P.: Whole-watershed mercury balance at Sagehen Creek, Sierra Nevada, Ca, Geochim. Cosmochim. Ac., 75, 2379–2392, doi:10.1016/j.gca.2011.01.041, 2011.

Feichter, J., Brost, R. A., and Heimann, M.: 3-Dimensional modeling of the concentration and deposition of Pb-210 aerosols, J. Geophys. Res., 96, 22447–22460, doi:10.1029/91jd02354, 1991.

Friedli, H. R., Radke, L. F., Lu, J. Y., Banic, C. M., Leaitch, W. R., and MacPherson, J. I.: Mercury emissions from burning of biomass from temperate North American forests: Laboratory and airborne measurements, Atmos. Environ., 37, 253–267, doi:10.1016/s1352-2310(02)00819-1, 2003a.

Friedli, H. R., Radke, L. F., Prescott, R., Hobbs, P. V., and Sinha, P.: Mercury emissions from the August 2001 wildfires in Washington State and an agricultural waste fire in Oregon and atmospheric mercury budget estimates, Global Biogeochem. Cy., 17, 1039, doi:10.1029/2002gb001972, 2003b.

Galarneau, E., Bidleman, T. F., and Blanchard, P.: Seasonality and interspecies differences in particle/gas partitioning of PAHs observed by the Integrated Atmospheric Deposition Network (IADN), Atmos. Environ., 40, 182–197, doi:10.1016/j.atmosenv.2005.09.034, 2006.

Gildemeister, A. E., Graney, J., and Keeler, G. J.: Source proximity reflected in spatial and temporal variability in particle and vapor phase Hg concentrations in Detroit, MI, Atmos. Environ., 39, 353–358, doi:10.1016/j.atmosenv.2004.08.052, 2005.

Gustin, M. and Jaffe, D.: Reducing the uncertainty in measurement and understanding of mercury in the atmosphere, Environ. Sci. Technol., 44, 2222–2227, doi:10.1021/es902736k, 2010.

Hedgecock, I. M. and Pirrone, N.: Mercury and photochemistry in the marine boundary layer-modeling studies suggest the in situ production of reactive gas phase mercury, Atmos. Environ., 35, 3055–3062, doi:10.1016/s1352-2310(01)00109-1, 2001.

ACPD
11, 29441–29477, 2011

Holmes, C. D., Jacob, D. J., Mason, R. P., and Jaffe, D. A.: Sources and deposition of reactive gaseous mercury in the marine atmosphere, Atmos. Environ., 43, 2278–2285, doi:10.1016/j.atmosenv.2009.01.051, 2009.

Holmes, C. D., Jacob, D. J., Corbitt, E. S., Mao, J., Yang, X., Talbot, R., and Slemr, F.: Global atmospheric model for mercury including oxidation by bromine atoms, Atmos. Chem. Phys., 10, 12037–12057, doi:10.5194/acp-10-12037-2010, 2010.

Hynes, A., Donohoue, D., Goodsite, M., Hedgecock, I., Pirrone, N., and Mason, R.: Our current understanding of major chemical and physical processes affecting mercury dynamics in the atmosphere and at air-water/terrestrial interfaces, in: Mercury Fate and Transport in the Global Atmosphere, edited by: Pirrone, N. and Mason, R. P., chap. 14, Springer, 2009.

Keeler, G., Glinsorn, G., and Pirrone, N.: Particulate mercury in the atmosphere – its significance, transport, transformation and sources, Water Air Soil Poll., 80, 159–168, doi:10.1007/bf01189664, 1995.

Keeler, G. J., Gratz, L. E., and Al-Wali, K.: Long-term atmospheric mercury wet deposition at Underhill, Vermont, Ecotoxicology, 14, 71–83, doi:10.1007/s10646-004-6260-3, 2005.

Koch, D. M., Jacob, D. J., and Graustein, W. C.: Vertical transport of tropospheric aerosols as indicated by Be-7 and Pb-210 in a chemical tracer model, J. Geophys. Res., 101, 18651–18666, doi:10.1029/96jd01176, 1996.

Kos, G., Ryzhkov, A., and Dastoor, A.: Analysis of uncertainties in measurements and mode for oxidised and particle-bound mercury, 10th International Conference on Mercury as a Global Pollutant, Halifax, Nova Scotia, Canada, 2011.

Lamborg, C. H., Fitzgerald, W. F., Vandal, G. M., and Rolfhus, K. R.: Atmospheric mercury in northern Wisconsin – sources and species, Water Air Soil Poll., 80, 189–198, doi:10.1007/bf01189667, 1995.

Landis, M. S., Stevens, R. K., Schaedlich, F., and Prestbo, E. M.: Development and characterization of an annular denuder methodology for the measurement of divalent inorganic reactive gaseous mercury in ambient air, Environ. Sci. Technol., 36, 3000–3009, doi:10.1021/es015887t, 2002.

Levine, S. Z. and Schwartz, S. E.: In-cloud and below-cloud scavenging of nitric acid vapor, Atmos. Environ., 16, 1725–1734, 1982.

Lin, C. J., Pongprueksa, P., Lindberg, S. E., Pehkonen, S. O., Byun, D., and Jang, C.: Scientific uncertainties in atmospheric mercury models I: Model science evaluation, Atmos. Environ., 40, 2911–2928, doi:10.1016/j.atmosenv.2006.01.009, 2006.

ACPD
11, 29441–29477, 2011

Lindberg, S. E. and Stratton, W. J.: Atmospheric mercury speciation: Concentrations and behavior of reactive gaseous mercury in ambient air, Environ. Sci. Technol., 32, 49–57, doi:10.1021/es970546u, 1998.
Lindberg, S., Bullock, R., Ebinghaus, R., Engstrom, D., Feng, X. B., Fitzgerald, W., Pirrone, N., Prestbo, E., and Seigneur, C.: A synthesis of progress and uncertainties in attributing the sources of mercury in deposition, Ambio, 36, 19–32, 2007.
Lindqvist, O. and Rodhe, H.: Atmospheric mercury – a review, Tellus B, 37, 136–159, 1985.
Liu, H. Y., Jacob, D. J., Bey, I., and Yantosca, R. M.: Constraints from Pb-210 and Be-7 on wet deposition and transport in a global three-dimensional chemical tracer model driven by assimilated meteorological fields, J. Geophys. Res., 106, 12109–12128, doi:10.1029/2000jd900839, 2001.
Lohman, K., Seigneur, C., Edgerton, E., and Jansen, J.: Modeling mercury in power plant plumes, Environ. Sci. Technol., 40, 3848–3854, doi:10.1021/es051556v, 2006.
Lombard, M. A. S., Bryce, J. G., Mao, H., and Talbot, R.: Mercury deposition in Southern New Hampshire, 2006–2009, Atmos. Chem. Phys., 11, 7657–7668, doi:10.5194/acp-11-7657-2011, 2011.
Lyman, S. N., Gustin, M. S., Prestbo, E. M., and Marsik, F. J.: Estimation of dry deposition of atmospheric mercury in Nevada by direct and indirect methods, Environ. Sci. Technol., 41, 1970–1976, doi:10.1021/es062323m, 2007.
Lyman, S. N., Gustin, M. S., Prestbo, E. M., Kilner, P. I., Edgerton, E., and Hartsell, B.: Testing and application of surrogate surfaces for understanding potential gaseous oxidized mercury dry deposition, Environ. Sci. Technol., 43, 6235–6241, 2009.
Lyman, S. N. and Gustin, M. S.: Determinants of atmospheric mercury concentrations in Reno, Nevada, USA, Sci. Total Environ., 408, 431–438, doi:10.1016/j.scitotenv.2009.09.045, 2009.
Lyman, S. N., Jaffe, D. A., and Gustin, M. S.: Release of mercury halides from KCl denuders in the presence of ozone, Atmos. Chem. Phys., 10, 8197–8204, doi:10.5194/acp-10-8197-2010, 2010.
Lynam, M. M. and Keeler, G. J.: Artifacts associated with the measurement of particulate mercury in an urban environment: The influence of elevated ozone concentrations, Atmos. Environ., 39, 3081–3088, doi:10.1016/j.atmosenv.2005.01.036, 2005
Mahaffey, K. R., Clickner, R. P., and Bodurow, C. C.: Blood organic mercury and dietary mercury intake: National health and nutrition examination survey, 1999 and 2000, Environ. Health Persp., 112, 562–570, 2004.

ACPD
11, 29441–29477, 2011

Mahaffey, K. R., Clickner, R. P., and Jeffries, R. A.: Adult women's blood mercury concentrations vary regionally in the United States: Association with patterns of fish consumption (NHANES 1999–2004), Environ. Health Persp., 117, 47–53, doi:10.1289/ehp.11674, 2009.

Malcolm, E. G. and Keeler, G. J.: Evidence for a sampling artifact for particulate-phase mercury in the marine atmosphere, Atmos. Environ., 41, 3352–3359, doi:10.1016/j.atmosenv.2006.12.024, 2007.

Mao, H., Talbot, R. W., Sigler, J. M., Sive, B. C., and Hegarty, J. D.: Seasonal and diurnal variations of Hg(0) over New England, Atmos. Chem. Phys., 8, 1403–1421, doi:10.5194/acp-8-1403-2008, 2008.

Mao, H., Talbot, R., Hegarty, J., and Koermer, J.: Speciated mercury at marine, coastal, and inland sites in New England – Part 2: Relationships with atmospheric physical parameters, Atmos. Chem. Phys. Discuss., 11, 28395–28443, doi:10.5194/acpd-11-28395-2011, 2011.

Mergler, D., Anderson, H. A., Chan, L. H. M., Mahaffey, K. R., Murray, M., Sakamoto, M., and Stern, A. H.: Methylmercury exposure and health effects in humans: A worldwide concern, Ambio, 36, 3–11, 2007.

Muramatsu, H., Yoshizawa, S., Abe, T., Ishii, T., Wada, M., Horiuchi, Y., and Kanekatsu, R.: Variation of Be-7 concentration in surface air at Nagano, Japan, J. Radioanal. Nucl. Ch., 275, 299–307, doi:10.1007/s10967-007-7056-8, 2008.

National Atmospheric Deposition Program: Mercury Deposition Network (MDN): A NADP Network, available at: http://nadp.sws.uiuc.edu/MDN/, 2011.

Odum, J. R., Hoffmann, T., Bowman, F., Collins, D., Flagan, R. C., and Seinfeld, J. H.: Gas/particle partitioning and secondary organic aerosol yields, Environ. Sci. Technol., 30, 2580–2585, doi:10.1021/es950943+, 1996.

Pacyna, E. G., Pacyna, J. M., Sundseth, K., Munthe, J., Kindbom, K., Wilson, S., Steenhuisen, F., and Maxson, P.: Global emission of mercury to the atmosphere from anthropogenic sources in 2005 and projections to 2020, Atmos. Environ., 44, 2487–2499, doi:10.1016/j.atmosenv.2009.06.009, 2010.

Pankow, J. F.: Review and comparative-analysis if the theories on partitioning between the gas and aerosol particulate phases in the atmosphere, Atmos. Environ., 21, 2275–2283, doi:10.1016/0004-6981(87)90363-5, 1987.

Pankow, J. F., Storey, J. M. E., and Yamasaki, H.: Effects of relative-humidity on gas-particle partitioning of semivolatile organic-compounds to urban particulate matter, Environ. Sci. Technol., 27, 2220–2226, doi:10.1021/es00047a032, 1993.

ACPD
11, 29441–29477, 2011

Pankow, J. F.: An absorption-model of the gas aerosol partitioning involved in the formation of secondary organic aerosol, Atmos. Environ., 28, 189–193, doi:10.1016/1352-2310(94)90094-9, 1994.
Petersen, G., Munthe, J., Pleijel, K., Bloxam, R., and Kumar, A. V.: A comprehensive Eulerian modeling framework for airborne mercury species: Development and testing of the tropospheric chemistry module (TCM), Atmos. Environ., 32, 829–843, doi:10.1016/s1352-2310(97)00049-6, 1998.
Poissant, L., Pilote, M., Xu, X. H., Zhang, H., and Beauvais, C.: Atmospheric mercury speciation and deposition in the Bay St. Francois wetlands, J. Geophys. Res., 109, D11301, doi:10.1029/2003jd004364, 2004.
Rutter, A. P. and Schauer, J. J.: The impact of aerosol composition on the particle to gas partitioning of reactive mercury, Environ. Sci. Technol., 41, 3934–3939, doi:10.1021/es062439i, 2007a.
Rutter, A. P. and Schauer, J. J.: The effect of temperature on the gas-particle partitioning of reactive mercury in atmospheric aerosols, Atmos. Environ., 41, 8647–8657, doi:10.1016/j.atmosenv.2007.07.024, 2007b.
Rutter, A. P., Hanford, K. L., Zwers, J. T., Perillo-Nicholas, A. L., Schauer, J. J., and Olson, M. L.: Evaluation of an offline method for the analysis of atmospheric reactive gaseous mercury and particulate mercury, J. Air Waste Manage. Assoc., 58, 377–383, doi:10.3155/1047-3289.58.3.377, 2008a.
Rutter, A. P., Schauer, J. J., Lough, G. C., Snyder, D. C., Kolb, C. J., Von Klooster, S., Rudolf, T., Manolopoulos, H., and Olson, M. L.: A comparison of speciated atmospheric mercury at an urban center and an upwind rural location, J. Environ. Monitor., 10, 102–108, doi:10.1039/b710247j, 2008b.
Sakata, M. and Marumoto, K.: Formation of atmospheric particulate mercury in the Tokyo metropolitan area, Atmos. Environ., 36, 239–246, doi:10.1016/s1352-2310(01)00432-0, 2002.
Sanei, H., Outridge, P. M., Goodarzi, F., Wang, F., Armstrong, D., Warren, K., and Fishback, L.: Wet deposition mercury fluxes in the canadian sub-arctic and southern alberta, measured using an automated precipitation collector adapted to cold regions, Atmos. Environ., 44, 1672–1681, doi:10.1016/j.atmosenv.2010.01.030, 2010.
Scheulhammer, A. M., Meyer, M. W., Sandheinrich, M. B., and Murray, M. W.: Effects of environmental methylmercury on the health of wild birds, mammals, and fish, Ambio, 36, 12–18,

ACPD
11, 29441–29477, 2011

doi:10.1579/0044-7447(2007)36[12:eoemot]2.0.co;2, 2007.
Schroeder, W. H. and Munthe, J.: Atmospheric mercury – an overview, Atmos. Environ., 32, 809–822, doi:10.1016/s1352-2310(97)00293-8, 1998.
Seigneur, C., Abeck, H., Chia, G., Reinhard, M., Bloom, N. S., Prestbo, E., and Saxena, P.: Mercury adsorption to elemental carbon (soot) particles and atmospheric particulate matter, Atmos. Environ., 32, 2649–2657, doi:10.1016/s1352-2310(97)00415-9, 1998.
Seigneur, C., Karamchandani, P., Lohman, K., Vijayaraghavan, K., and Shia, R. L.: Multiscale modeling of the atmospheric fate and transport of mercury, J. Geophys. Res.-Atmos., 106, 27795–27809, doi:10.1029/2000jd000273, 2001.
Seigneur, C., Karamchandani, P., Vijayaraghavan, K., Lohman, K., Shia, R. L., and Levin, L.: On the effect of spatial resolution on atmospheric mercury modeling, Sci. Total Environ., 304, 73–81, doi:10.1016/s0048-9697(02)00558-2, 2003.
Seinfeld, J. H. and Pandis, S. N.: Atmospheric chemistry and physics: From air pollution to climate change, 2nd ed., John Wiley & Sons, Inc., 1203 pp., 2006.
Selin, N. E., Jacob, D. J., Park, R. J., Yantosca, R. M., Strode, S., Jaegle, L., and Jaffe, D.: Chemical cycling and deposition of atmospheric mercury: Global constraints from observations, J. Geophys. Res., 112, D02308, doi:10.1029/2006jd007450, 2007.
Selin, N. E. and Jacob, D. J.: Seasonal and spatial patterns of mercury wet deposition in the United States: Constraints on the contribution from North American anthropogenic sources, Atmos. Environ., 42, 5193–5204, 2008.
Selin, N. E., Jacob, D. J., Yantosca, R. M., Strode, S., Jaegle, L., and Sunderland, E. M.: Global 3-D land-ocean-atmosphere model for mercury: Present-day versus preindustrial cycles and anthropogenic enrichment factors for deposition, Global Biogeochem. Cy., 22, Gb3099, doi:10.1029/2008gb003282, 2008.
Sheffield, A. E. and Pankow, J. F.: Specific surface-area of urban atmospheric particulate matter in Portland, Oregon, Environ. Sci. Technol., 28, 1759–1766, doi:10.1021/es00058a030, 1994.
Sigler, J. M., Mao, H., and Talbot, R.: Gaseous elemental and reactive mercury in Southern New Hampshire, Atmos. Chem. Phys., 9, 1929–1942, doi:10.5194/acp-9-1929-2009, 2009.
Skov, H., Brooks, S. B., Goodsite, M. E., Lindberg, S. E., Meyers, T. P., Landis, M. S., Larsen, M. R. B., Jensen, B., McConville, G., and Christensen, J.: Fluxes of reactive gaseous mercury measured with a newly developed method using relaxed eddy accumulation, Atmos. Environ., 40, 5452–5463, doi:10.1016/j.atmosenv.2006.04.061, 2006.

ACPD
11, 29441–29477, 2011

Soerensen, A. L., Sunderland, E. M., Holmes, C. D., Jacob, D. J., Yantosca, R. M., Skov, H., Christensen, J. H., Strode, S. A., and Mason, R. P.: An improved global model for air-sea exchange of mercury: High concentrations over the North Atlantic, Environ. Sci. Technol., 44, 8574–8580, doi:10.1021/es102032g, 2010.

Sunderland, E. M. and Mason, R. P.: Human impacts on open ocean mercury concentrations, Global Biogeochem. Cy., 21, Gb4022, doi:10.1029/2006gb002876, 2007.

Swartzendruber, P. C., Jaffe, D. A., Prestbo, E. M., Weiss-Penzias, P., Selin, N. E., Park, R., Jacob, D. J., Strode, S., and Jaegle, L.: Observations of reactive gaseous mercury in the free troposphere at the Mount Bachelor Observatory, J. Geophys. Res., 111, D24302, doi:10.1029/2006jd007415, 2006.

Talbot, R., Mao, H., Feddersen, D., Smith, M., Kim, S. Y., Sive, B. C., Haase, K., Ambrose, J., Zhou, Y., and Russo, R.: Comparison of particulate mercury measured with manual and automated methods, Atmosphere, 2, 1–20, doi:10.3390/atmos2010001, 2011.

ter Schure, A., Caffrey, J., Gustin, M. S., Holmes, C. D., Hynes, A., Landing, B., Landis, M. S., Laudel, D., Levin, L., Nair, U., Jansen, J., Ryan, J., Walters, J., Schauer, J. J., Volkamer, R., Waters, D., and Weiss, P.: An integrated approach to asses elevated mercury wet deposition and concentrations in the south eastern United States, 10th International Conference on Mercury as a Global Pollutant, Halifax, Nova Scotia, Canada, 2011.

Vijayaraghavan, K., Karamchandani, P., Seigneur, C., Balmori, R., and Chen, S. Y.: Plume-in-grid modeling of atmospheric mercury, J. Geophys. Res., 113, D24305, doi:10.1029/2008jd010580, 2008.

Wang, S. X., Zhang, L., Li, G. H., Wu, Y., Hao, J. M., Pirrone, N., Sprovieri, F., and Ancora, M. P.: Mercury emission and speciation of coal-fired power plants in China, Atmos. Chem. Phys., 10, 1183–1192, doi:10.5194/acp-10-1183-2010, 2010.

Wang, Q., Jacob, D. J., Fisher, J. A., Mao, J., Leibensperger, E. M., Carouge, C. C., Le Sager, P., Kondo, Y., Jimenez, J. L., Cubison, M. J., and Doherty, S. J.: Sources of carbonaceous aerosols and deposited black carbon in the Arctic in winter–spring: implications for radiative forcing, Atmos. Chem. Phys. Discuss., 11, 19395–19442, doi:10.5194/acpd-11-19395-2011, 2011.

Wang, Y. H., Jacob, D. J., and Logan, J. A.: Global simulation of tropospheric O_3-NO_x-hydrocarbon chemistry 1. Model formulation, J. Geophys. Res., 103, 10713–10725, doi:10.1029/98jd00158, 1998.

Weiss-Penzias, P., Gustin, M. S., and Lyman, S. N.: Observations of speciated atmospheric

ACPD
11, 29441–29477, 2011

mercury at three sites in Nevada: Evidence for a free tropospheric source of reactive gaseous mercury, J. Geophys. Res., 114, D14302, doi:10.1029/2008jd011607, 2009.
Weiss-Penzias, P. S., Gustin, M. S., and Lyman, S. N.: Sources of gaseous oxidized mercury and mercury dry deposition at two southeastern US sites, Atmos. Environ., 45, 4569–4579, doi:10.1016/j.atmosenv.2011.05.069, 2011.
Wesely, M. L.: Parameterization of surface resistances to gaseous dry deposition in regional-scale numerical-models, Atmos. Environ., 23, 1293–1304, doi:10.1016/0004-6981(89)90153-4, 1989.
Xiu, G. L., Cai, J., Zhang, W. Y., Zhang, D. N., Bueler, A., Lee, S. C., Shen, Y., Xu, L. H., Huang, X. J., and Zhang, P.: Speciated mercury in size-fractionated particles in Shanghai ambient air, Atmos. Environ., 43, 3145–3154, doi:10.1016/j.atmosenv.2008.07.044, 2009.
Yamasaki, H., Kuwata, K., and Miyamoto, H.: Effects of ambient temperature on aspects of airborne polycyclic aromatic hydrocarbons, Environ. Sci. Technol., 16, 189–194, doi:10.1021/es00098a003, 1982.
Yoshimori, M.: Beryllium 7 radionucleide as a tracer of vertical air mass transport in the troposphere, 36, Atmospheric Remote Sensing, 828–832, 2005.
Zhang, L., Jacob, D. J., Downey, N. V., Wood, D. A., Blewitt, D., Carouge, C. C., van Donkelaar, A., Jones, D. B. A., Murray, L. T., and Wang, Y.: Improved estimate of the policy-relevant background ozone in the United States using the GEOS-Chem global model with 1/2° × 2/3° horizontal resolution over North America, Atmos. Environ., 45, 6769–6776, 2011.
Zhang, Y., Jaegle, L., Holmes, C. D., Jacob, D. J., Van Donkelaar, A., and Martin, R.: Nested-grid modeling of mercury wet deposition over North America, 10th International Conference on Mercury as Global Pollutant, Halifax, Nova Scotia, Canada, 2011.

ACPD
11, 29441–29477, 2011

Table 1. Measurement sites for RGM and PBM

Site	Location	Record	$PM_{2.5}$ data[a]	Reference
Experimental Lakes Area, Ontario	49.7° N, 93.7° W	May 2005–Dec 2009	b	Graydon et al. (2008)
Milwaukee, Wisconsin	43.1° N, 87.8° W	Jul 2004–May 2005	c	Rutter and Schauer (2007b)
Outlying Landing Field, Pensacola, Florida	30.6° N, 87.4° W	Jan 2009–Dec 2009	c	Edgerton et al. (2006)
Reno, Nevada	39.3° N, 119.5° W	Feb 2007–Jan 2009	d	Lyman and Gustin (2009)
Thompson Farm, New Hampshire	43.1° N, 71.0° W	Jan 2009–Jun 2010	d	Sigler et al. (2009)

[a] All $PM_{2.5}$ data are 24-h averages.
[b] $PM_{2.5}$ from nearby Voyageurs National Park IMPROVE site (http://vista.cira.colostate.edu/IMPROVE/).
[c] $PM_{2.5}$ collocated with Hg measurements.
[d] $PM_{2.5}$ for Reno and Thompson Farm were obtained from the Environmental Protection Agency Air Quality System (http://www.epa.gov/ttn/airs/airsaqs).

ACPD
11, 29441–29477, 2011

Table 2. Regression coefficients for $\log_{10}(K^{-1}) = a + b/T$

Site[a]	a	b	r^2	Reference
Experimental Lakes	9 ± 4	−2400 ± 1100	0.57	this work
Milwaukee	7 ± 2	−1900 ± 400	0.43	this work
Pensacola	6 ± 2	−1600 ± 600	0.16	this work
Reno	13 ± 2	−3300 ± 600	0.54	this work
Thompson Farm	8 ± 6	−2000 ± 1600	0.33	this work
All sites (combined)	10 ± 1	−2500 ± 300	0.49	this work
Urban[b,c]	15 ± 2	−4250 ± 480	0.77	Rutter and Schauer (2007b)
Urban[d]	7 ± 1	−1710 ± 380	0.49	Rutter and Schauer (2007b)
Laboratory, $HgCl_2$ on $(NH_4)_2\ SO_4$[e]	19 ± 2	−5720 ± 470	0.99	Rutter and Schauer (2007b)
Laboratory, $HgCl_2$ on adipic acid and $HgCl_2$[e]	9 ± 1	−2780 ± 240	0.96	Rutter and Schauer (2007b)

[a]Measurements of RGM and PBM were made by Tekran instruments unless otherwise indicated.
[b]Hg collected using filter-based methods (Rutter and Schauer, 2007a, b).
[c]Milwaukee (Jul 2004–May 2005) and Riverside, California (16 Jul–7 Aug 2005) (Rutter and Schauer,2007b).
[d]Milwaukee (Jul 2004–May 2005) (Rutter and Schauer, 2007b).
[e]Dry conditions (RH < 1 %)

ACPD
11, 29441–29477, 2011

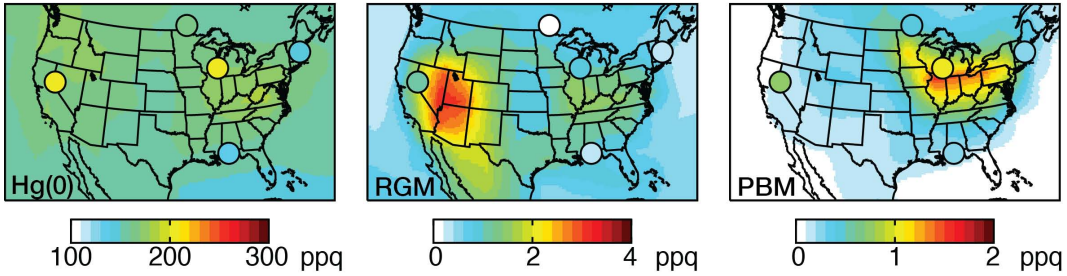

Fig. 1. Simulated (background solid contours) and observed (circles) annual mean concentrations of speciated Hg. Measurement sites and measurement periods are listed in Table 1. Model results are for 2007–2009.

ACPD
11, 29441–29477, 2011

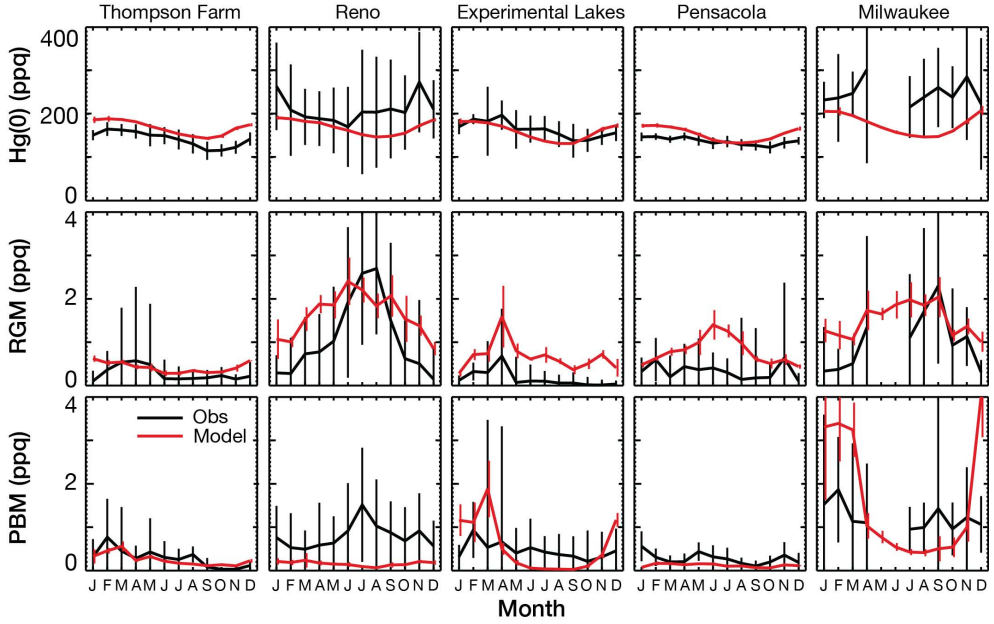

Fig. 2. Monthly mean observed (black, $\pm 1\sigma$) and simulated (red, $\pm 1\sigma$) concentrations of speciated Hg during daytime hours (10:00–16:00 local time). Standard deviations for simulated Hg(0) are less than the width of the line. Measurement sites and measurement periods are listed in Table 1. Each month contain at least two weeks of daily measurements. Model results are for 2007–2009.

ACPD
11, 29441–29477, 2011

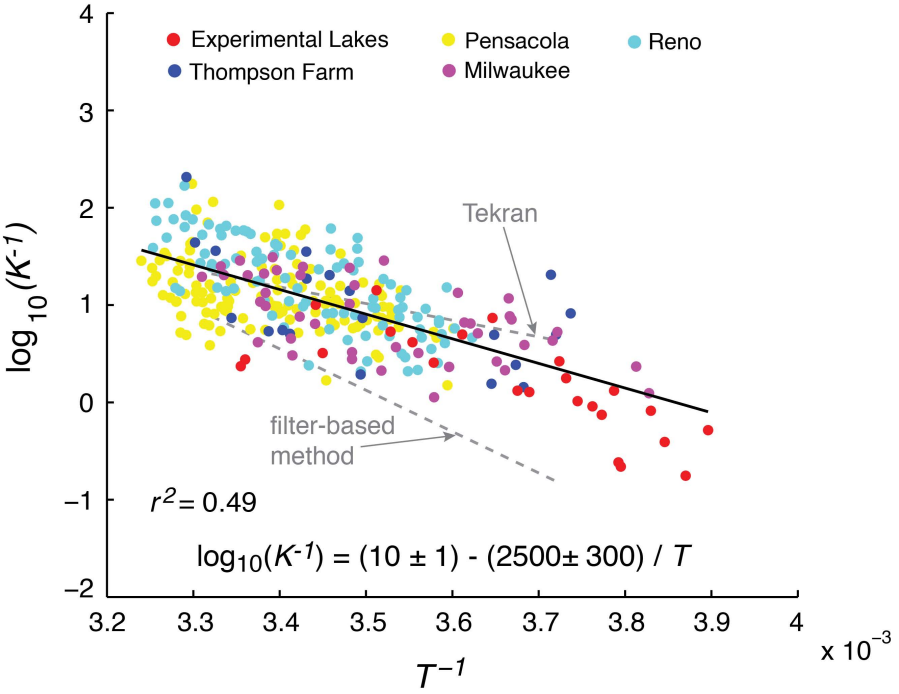

Fig. 3. Temperature dependence of the relationship between gas-phase and particle-phase mercury as defined by Eqs. (1) and (2). Each point represents one observation day (10:00–16:00 local time) for the color-coded sites in Table 1. Days with RGM or PBM below 0.34 ppq, or $PM_{2.5}$ below 2 $\mu g\,m^{-3}$ are rejected as below analytical detection limits. Temperature is in K. Also shown is the least-squares regression line (solid) and the regression parameters with 95 % bootstrapped confidence intervals (legend). Shown in dashed grey are the least-squares regression lines from Rutter and Schauer (2007b) for urban data collected using a filter-based method and a Tekran instrument.

ACPD
11, 29441–29477, 2011

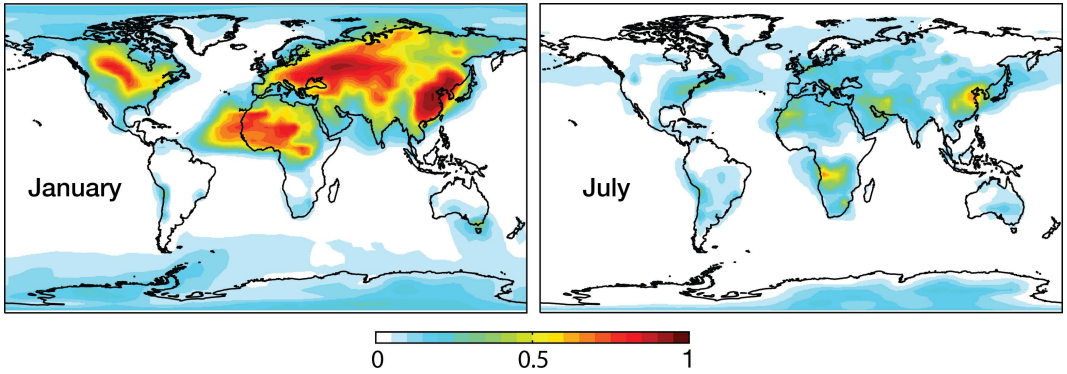

Fig. 4. Mean fraction of Hg(II) partitioned into the particle phase in surface air in January and July. Values are 2007–2009 GEOS-Chem model results obtained using Eqs. (1) and (2), not including partitioning into sea-salt aerosol which is treated separately following Holmes et al. (2010).

ACPD
11, 29441–29477, 2011

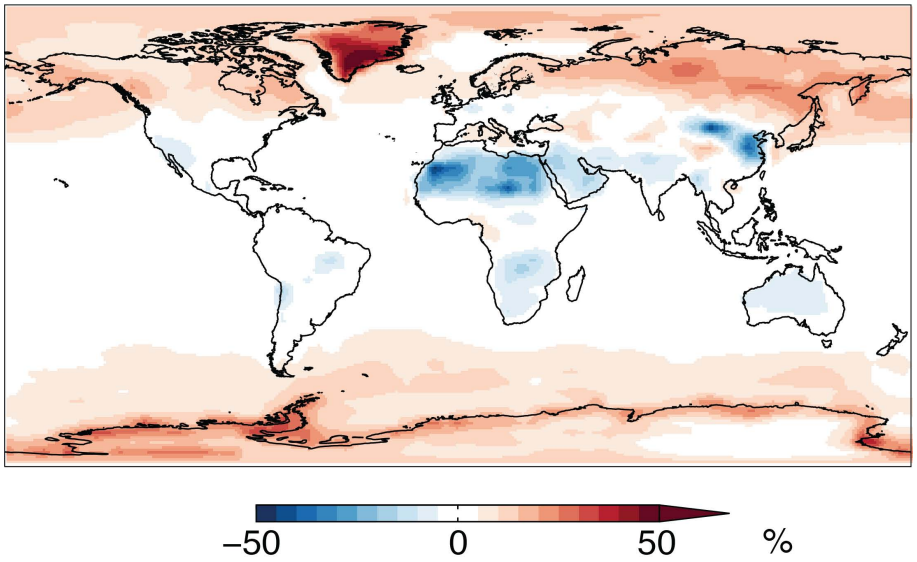

Fig. 5. Percent difference in total annual Hg(II) deposition between our standard simulation and a simulation where all Hg(II) is assumed to deposit as gas. Positive values indicate higher deposition in the standard simulation.

ACPD
11, 29441–29477, 2011

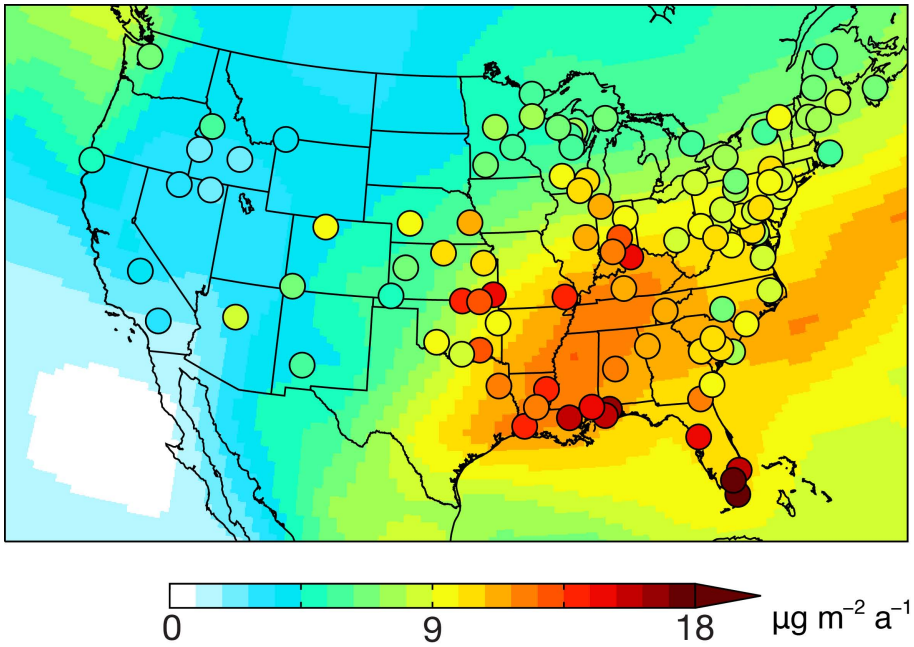

Fig. 6. Annual Hg wet deposition fluxes for 2007–2009. Model results (solid contours) are compared to measurements (circles) from the Mercury Deposition Network (MDN). The MDN observations have been averaged as in Holmes et al. (2010).

ACPD
11, 29441–29477, 2011

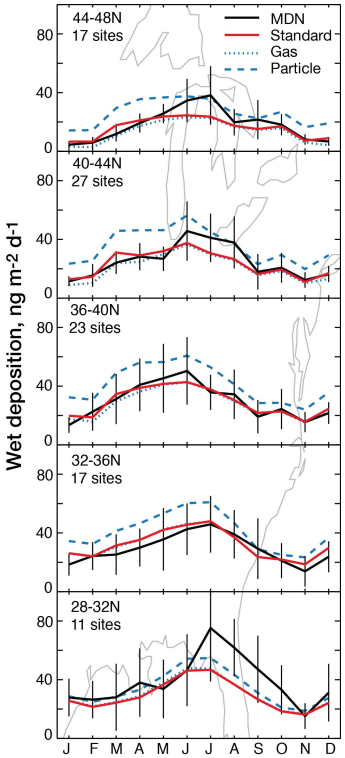

Fig. 7. Seasonal variation of Hg wet deposition fluxes in the eastern US for different latitude bands. Values are monthly means for 2007–2009 in the observations (black) and in the model (red, blue). Observations from Fig. 6 are averaged over all sites in the latitude band that meet data density criteria described by Holmes et al. (2010). Model results are sampled at the same sites and are shown for the standard simulation (red) and for sensitivity simulations where all Hg(II) is assumed to deposit as a gas (blue dotted) or as a particle (blue dashed). Standard deviations are calculated from monthly means for individual MDN sites and individual years.

ACPD
11, 29441–29477, 2011